

Earth Observation for the Arctic: The Tana River

Vesa Keto & Sampsa Koponen

Reports of the Finnish Environment Institute 39 / 2022

Earth Observation for the Arctic: The Tana River

Vesa Keto & Sampsa Koponen



Reports of the Finnish Environment Institute 39 | 2022
Finnish Environment Institute
Data and information centre

Authors: Vesa Keto & Sampsa Koponen

Subject Editor: Ahti Lepistö

Financier/commissioner: Ministry for Foreign Affairs of Finland & The Finnish Ministry of Environment
Publisher and financier of publication: Finnish Environment Institute (SYKE)
Latokartanonkaari 11, 00790 Helsinki, Finland, Phone +358 295 251 000, syke.fi

Layout: Pirkko Väänänen & Sampsa Koponen

Cover photo: USGS / NASA Landsat Program, SYKE (2018)

The publication is available in the internet (pdf): syke.fi/publications | helda.helsinki.fi/syke

ISBN 978-952-11-5523-9 (PDF)

ISSN 1796-1726 (online)

Year of issue: 2022

Abstract

Earth Observation for the Arctic: The Tana River

Satellite Earth Observation methods can be used to monitor the environment with extensive spatial and temporal coverage. The Sentinel satellites of Copernicus programme of the European Union provide an excellent opportunity to develop monitoring systems for the Arctic. This report shows visual examples where satellite images have been used to provide information about River Tana located in Northern Finland and Norway. The visual snow and ice cover examples cover different seasons over the year: from the winter to the low water season of the late summer.

The proposed next steps are to extend the use of EO methods into efficient routine use for monitoring the arctic environment. Provision of EO-based lake ice, snow cover and water quality information is already on going and partially automated. Additional effort is needed especially on the further processing of EO-based information, user collaboration and on identification of the barriers.

Keywords: Earth observation, environment, monitoring, Sentinel satellites, Copernicus programme, water quality, water surface temperature, snow cover, ice cover

Tiivistelmä

Arktisen alueen satelliittihavainnointi: esimerkkejä Tenojoelta

Satelliittihavaintomenetelmien avulla ympäristön tilaa on mahdollista seurata hyvällä alueellisella ja ajallisella erotuskyvyllä. Euroopan Unionin Copernicus ohjelman Sentinel satelliitit tarjoavat oivallisen tilaisuuden rakentaa kattava seurantajärjestelmä arktiselle alueelle. Tämä raportti keskittyy Pohjois-Suomessa ja Norjassa olevan Tenojoen tilanteen seurantaan satelliittikuvien avulla eri vuodenaikoina. Esimerkit kuvaavat joen tilaa lumi ja jääpeitteisestä talvesta loppukesän vähävetiseen kauteen.

Jatkovaiheiksi ehdotetaan satelliittihavaintomenetelmien käyttöönottoa osana arktisen ympäristön jatkuvaluonteista seuranta. Satelliittihavaintopohjaisia järvien jääpeitetietoja, lumenpeittävyyttä ja vedenlaatutietoja tuotetaan jo osin automatisoidusti. Kehitystyötä tarvitaan erityisesti aineistojen jatkojalostamiseksi ja käyttäjäyhteistyön tiivistämiseksi.

Asiasanat: Satelliittihavainnointi, kaukokartoitus, ympäristö, seuranta, Sentinel satelliitit, Copernicus-ohjelma, vedenlaatu, pintalämpötila, lumipeite, jääpeite

Sammandrag

Jordobservation av Arktis: Tana älv

Metoder för observationssatelliter kan användas för att övervaka miljön med god rumslig och tidsmässig täckning. Sentinel-satelliterna i Europeiska unionens Copernicus-program ger en utmärkt möjlighet att utveckla ett omfattande övervakningssystem för det arktiska området. Denna rapport fokuserar på att följa läget i Tana älv, som ligger i norra Finland och Norge, med hjälp av satellitbilder under olika årstider. Exempelen i rapporten beskriver läget i älv från att den är täckt av snö- och is på vintern till sensommarens lågvattensåsong.

De föreslagna nästa stegen är att göra metoderna för jordobservationssatelliter till en del av den rutinmässiga övervakningen av den arktiska miljön. Information om sjöars istäcke, snötäckning och vattenkvalitetsinformation produceras redan delvis automatiserat med hjälp av jordobservationssatelliter. Ytterligare ansträngningar behövs särskilt för vidarebearbetning av informationen från jordobservationssatelliter och för att stärka användarsamarbetet.

Nyckelord: Jordobservation, miljö, övervakning, Sentinel-satelliter, Copernicus-programmet, vattenkvalitet, vattentemperatur, snötäcke, istäcke

Preface

The Arctic region is experiencing large alterations due to climate change and other human activities. According to the Arctic Council, the magnitude of warming in the Arctic is twice as large as on the global scale (AMAP 2017). This is seen as less extensive snow cover, earlier ice melt and changing ecosystems which, in turn, threaten the livelihoods of local inhabitants. To understand these changes and to mitigate the impacts of the warming climate, extensive and frequent monitoring of the Arctic environment is needed.

Satellite Earth Observation (EO) techniques can gather environmental monitoring data with extensive temporal and spatial coverage. The Sentinel satellites of the Copernicus programme of the European Union observe the whole Arctic region every day, although cloud cover and darkness in the winter prevent part of the observations. This data source creates an excellent opportunity to develop monitoring systems for the Arctic.

The Finnish Environment Institute (SYKE) has been developing environmental EO applications since the mid-1990s. SYKE's current EO portfolio includes monitoring the water quality of lakes and the Baltic Sea, cryosphere (snow cover extent and lake ice extent), landcover and land use, and vegetation phenology. Many of these are publicly available through the TARKKA service of SYKE (TARKKA 2021).

This report was created during the project “ARWAT II, Arctic freshwater resources—Arctic council collaboration (part 2)”. The main objectives of the project were:

- to demonstrate the use of EO for providing information about the state and changes of Arctic water resources to other Arctic countries,
- to encourage the use of EO for Arctic monitoring, e.g., in the Arctic Monitoring and Assessment Programme (AMAP) and
- to promote the EO capabilities of the Finnish Environment Institute

The main findings of the project are available in the form of a storymap at: syke.fi/EOstorymap. This report presents a case for using EO methods to monitor the Tana River located in Northern Finland and Norway. We demonstrate how satellite images can provide information about the river in different seasons starting from the ice and snow cover of the winter, to the melting season of the spring and the low water season of the late summer.

This work has been funded by Ministry for Foreign Affairs of Finland and SYKE. The Finnish Ministry of Environment coordinated the work.

1.11.2022 Helsinki

Vesa Keto, Senior Developer, and Sampsa Koponen, Head of Unit, Finnish Environment Institute (SYKE)

Contents

Abstract.....	3
Tiivistelmä	4
Sammandrag	5
Preface	7
1 Introduction	9
1.1 The basics of EO.....	9
1.2 Purpose of the report.....	9
2 The River Tana	10
3 Wintertime – Snow cover.....	14
4 Early spring – Ice.....	18
5 Late spring – Plumes	21
6 Early summer – Warming water	25
7 Late summer – Retreating water	27
8 Further actions.....	32
Acronyms.....	33
References.....	34

1 Introduction

1.1 The basics of EO

Satellite instruments utilize a variety of techniques to observe the Earth. For example, optical EO instruments observe the light originating from the Sun and reflected from the target on the Earth's surface. Microwave instruments observe either radiation given off by the target (radiometers) or the sensor itself (radars). The selection of the instrument depends on the application. For example, radiometers are used to measure surface temperatures, whereas optical instruments are more suited for determining the water quality.

The signal captured by the instrument is converted into information about the target through various mathematical (methods called) algorithms. These vary from simple—such as band ratio algorithms calibrated with empirical coefficients—to very complex—such as bio-optical modelling and artificial neural networks. For many applications, these algorithms are available in various software packages and in the scientific literature. Local field measurements can be utilized to ensure that these EO products have sufficient accuracy and, in some cases, adjust or calibrate the EO values.

Many aquatic and terrestrial variables can be monitored from space. From marine and lake waters these include the presence and concentration of various substances such as phytoplankton (algal blooms), suspended inorganic material, and dissolved organic matter. In addition, it is possible to estimate the surface temperature of water and if it has ice or snow cover. Over land, it is possible to monitor the amount, type and seasonal changes of vegetation, buildings, roads, other man-made structures, and the extent of snow cover. In the atmosphere clouds, aerosols, the composition of gases can be monitored. It is important also to note that EO methods cannot observe parameters that do not have a clear effect on the measured electromagnetic signal. In the case of water quality, this includes, e.g., nutrients, bacteria, viruses, and toxins.

The characteristics of the satellite data are described in detail in syke.fi/EOstorymap. The most important elements include spatial resolution, temporal resolution and spectral characteristics. Spatial resolution defines the size of the smallest object that can be resolved in the image (from about 30 cm to about 1 km with current optical instruments). Temporal resolution or coverage defines the amount of time it takes for the instrument to make two consequent measurements of the target area. With current moderate spatial resolution instruments, it is possible to observe the globe in a day or two while with high resolution instruments this takes 5 to 10 days. The spectral characteristics define the wavelengths of the spectra that the instrument observes. The number of bands in current optical satellite instruments varies from a few to more than 200. The bands are placed on wavelengths where the strength of the reflected light depends on the properties of the target of interest. For example, vegetation has a strong reflectance in the infra-red part of the spectrum and weak reflectance in red. For water quality applications it is important to cover most of the visible and near-infrared wavelengths so that the processing steps can derive estimates of the parameters listed above.

1.2 Purpose of the report

This report aims to promote the use of EO methods to monitor the Arctic. The River Tana in Northern Finland and Norway is used as a target case and we show examples obtained in different seasons.

The report is targeted to policymakers (e.g., environment ministries), national and local environment agencies, and municipalities in all Arctic countries.

2 The River Tana

The *Tana River* is an arctic river meandering through the Lapland region of Finland and Norway at latitudes 68-70 degrees, well beyond the Arctic Circle (Figure 2). It collects waters from the surrounding catchment area and discharges into *Tanafjord* in the Barents Sea (Figure 1). The river mouth is one of Europe's largest river deltas, shaped by constantly evolving sand and mud banks as the meltwater runs off from the mountains surrounding the Tana river each spring. The river delta is protected by the *Tanamunningen* nature reserve.

The full length of the river is ca. 360 km, with the river width increasing towards the Barents Sea from less than 100 m to approximately 1 km at *Tanamunningen*. The area of the watershed for the river Tana is approximately 16,400 km² of which only 3% are lakes (ELY-centre for Lapland, 2010). With only a few lakes and marshlands connected to the watercourse, the river experiences a major portion of the meltwater runoff directly with no reservoirs acting as a buffer during the intensive snowmelt. This leads to strongly fluctuating water levels and high discharge rates each year.



Figure 1. Isometric view from North to South, Sentinel-2 (July 2017).

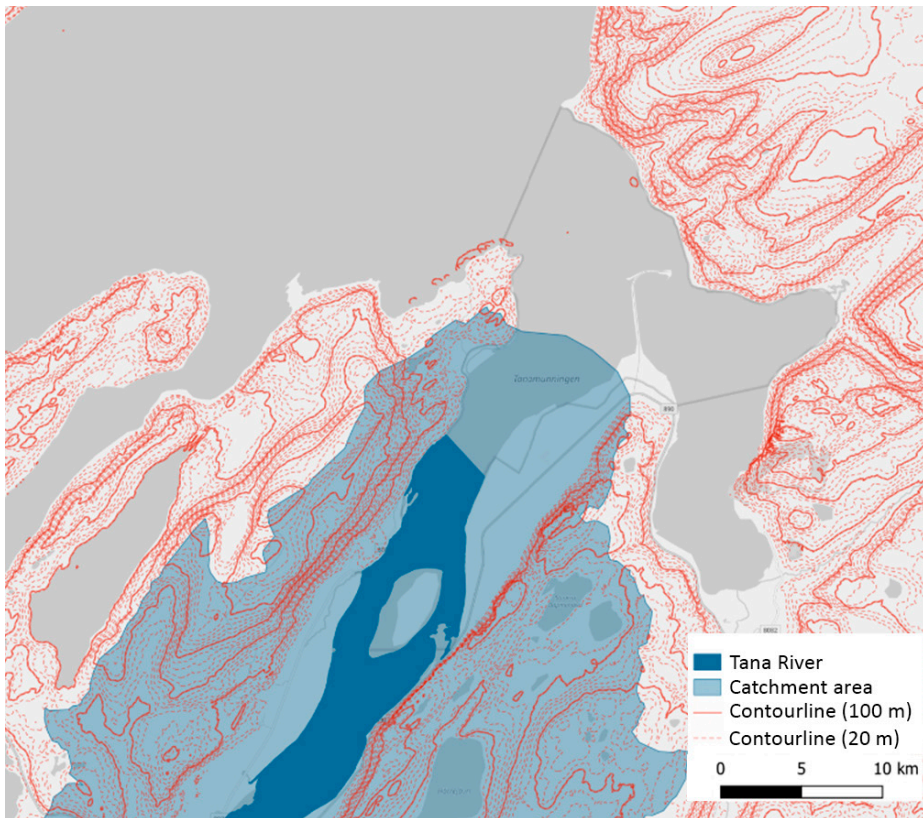
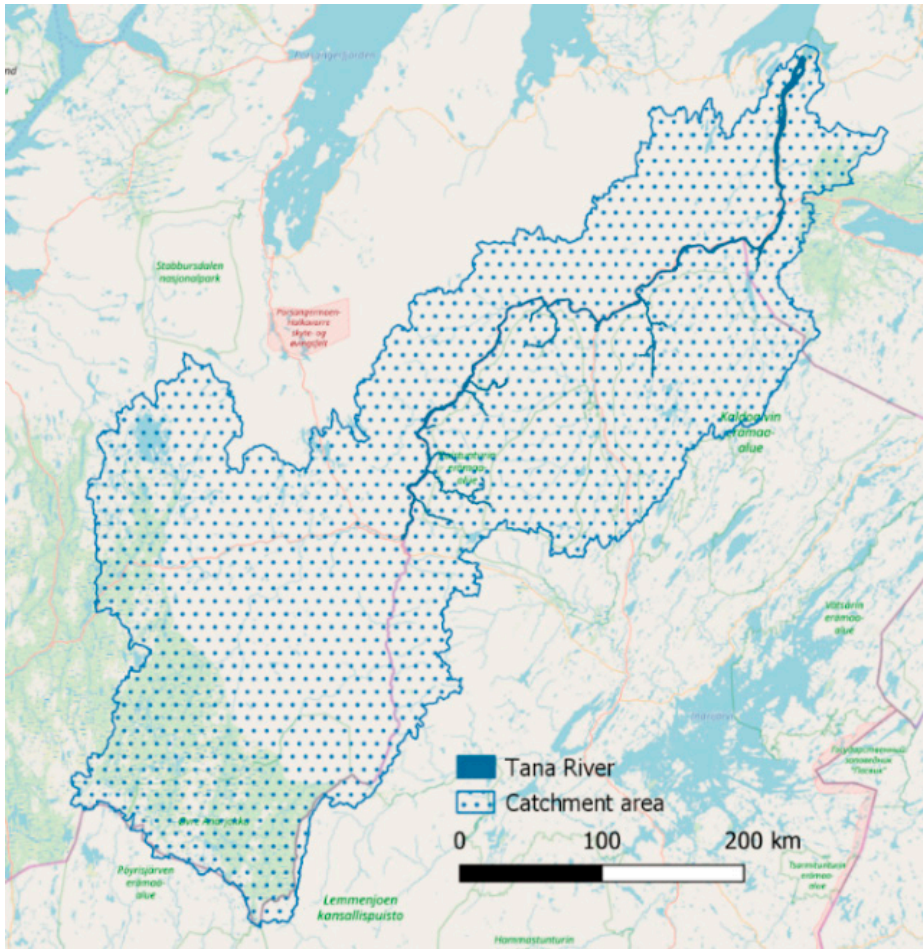


Figure 2. The catchment area of the Tana river (left), and a closeup of the topology at the river end, Tanamunnungen nature reservat (right).

During each year, the river undergoes multiple very distinct phases: complete ice cover through the winter, high flowrates during the melting period in spring and early summer, drying out during the late summer and finally freezing again for the next winter. The main forcing element for the dynamics is the snow mass accumulating through the winter over the river catchment area.

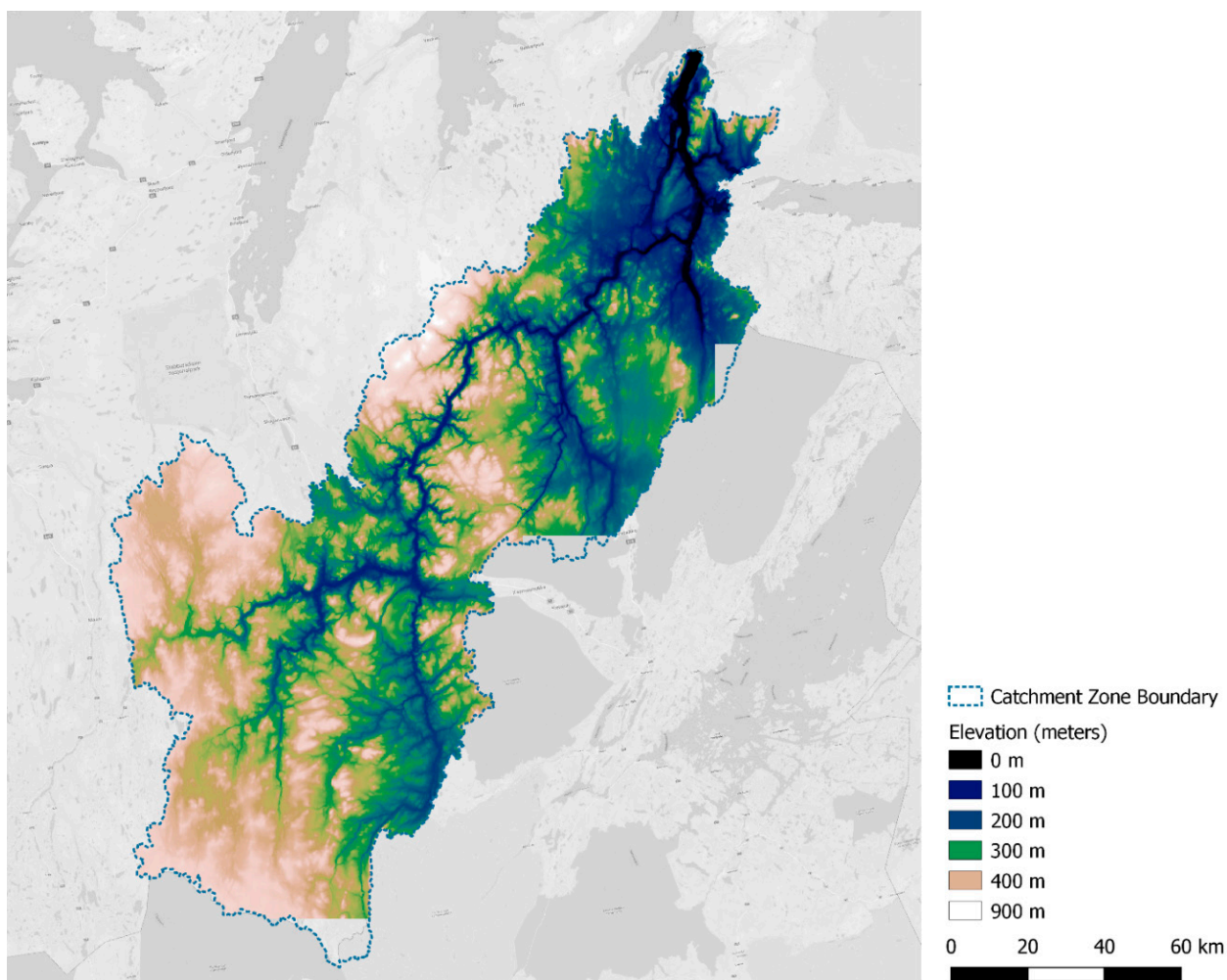


Figure 3. Terrain elevation zones of the Tana catchment.

The average temperatures at the riverside, at *Tana Bru*, range annually between -15 and +15 degrees Celsius (Figure 4). For the period 2014-2019, the minimum month-average air temperature for the wintertime has fluctuated by 9 Celsius between -16 and -7 degrees, while the summer peak temperatures have remained more stable.

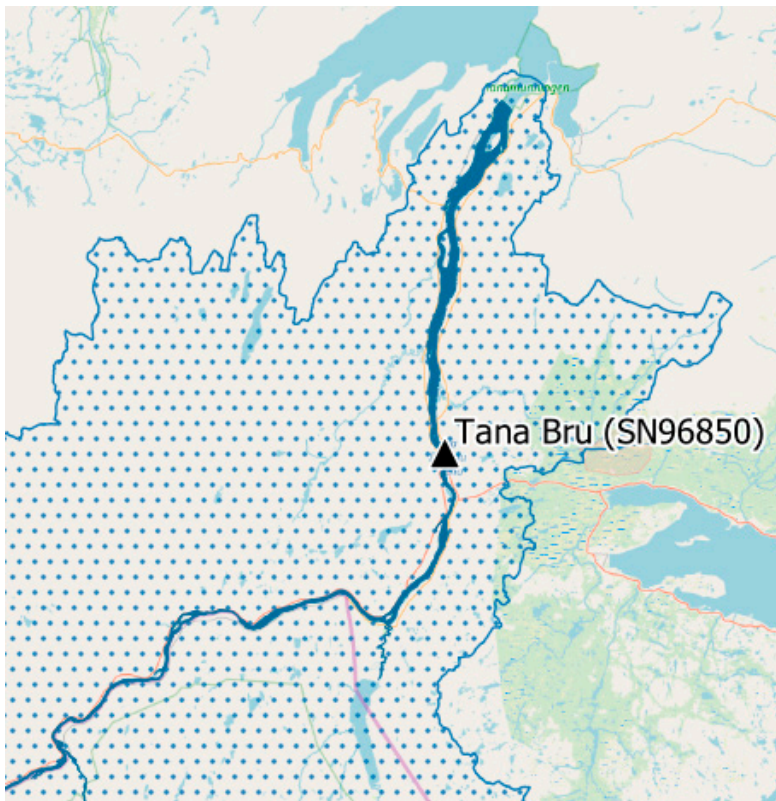
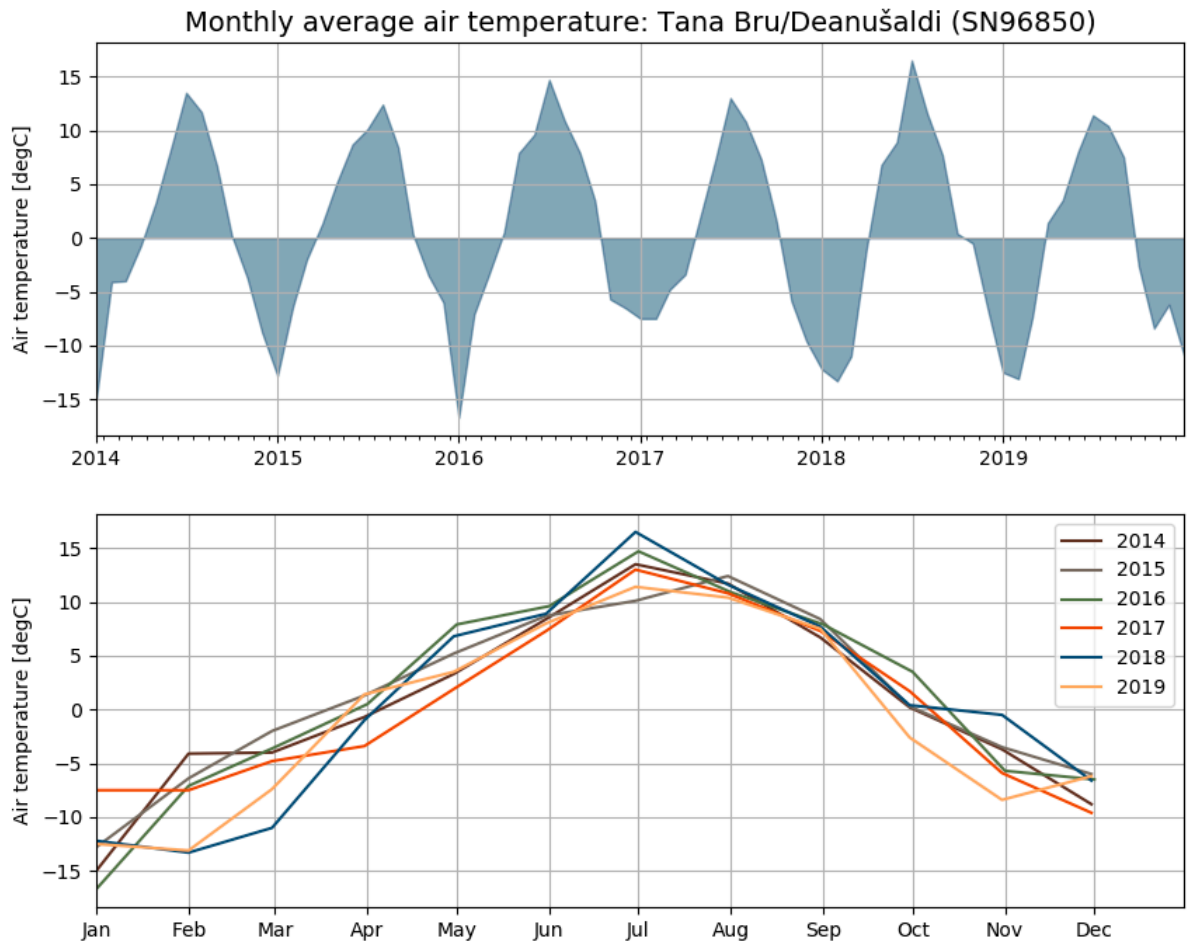


Figure 4. Monthly air temperature average measured at Tana Bru. Data from the Norwegian Meteorological Institute (MET Norway, 2020).

3 Wintertime – Snow cover

At the beginning of each year, Northern Fennoscandia experiences the polar night when the Sun does not rise above the horizon. Optical satellite instruments measure light reflected from the Earth's surface and cannot operate under these conditions. Starting approximately from February 20th, the Sun rises enough to enable optical observations within the latitudes of the Tana river (Figure 5).

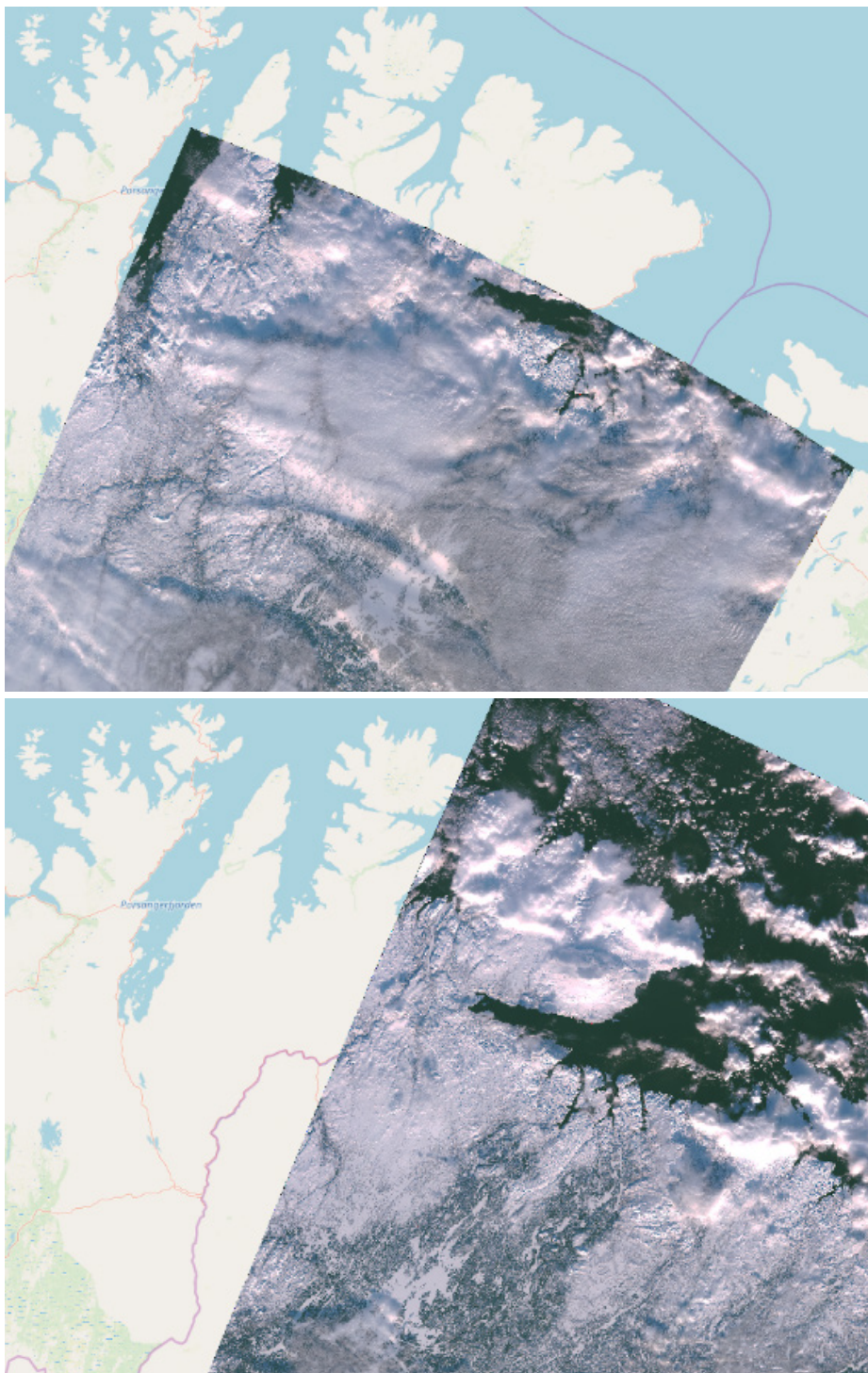


Figure 5. The northern limit of the area observed by the Sentinel-2 optical instruments on Feb 18 (above) and Feb 20 (below).

The snow accumulating over the catchment area of the river is a major force responsible for the different annual phases the river undergoes each year. The onset and duration of the melting period defines the forthcoming dynamics of the river, affects flooding risk (ELY-centre for Lapland, 2010) and determines the annual recharge of the groundwater reservoirs and finally the duration of the growing season of the nearby landscape. The long-term changes in snowmelt runoff in the Arctic region have also been considered a sensitive indicator of climate change.

The snow-covered areas are readily evident in the true-colour satellite images as white and bright areas over the landscape (Figure 6). The true colour imagery is generated by combining the reflections of red, green and blue light, which is a somewhat similar process to the formation of the images captured by our household digital cameras (True-colour satellite images, 2021). Almost all satellites which have optical instruments, provide data for generating true colour images.

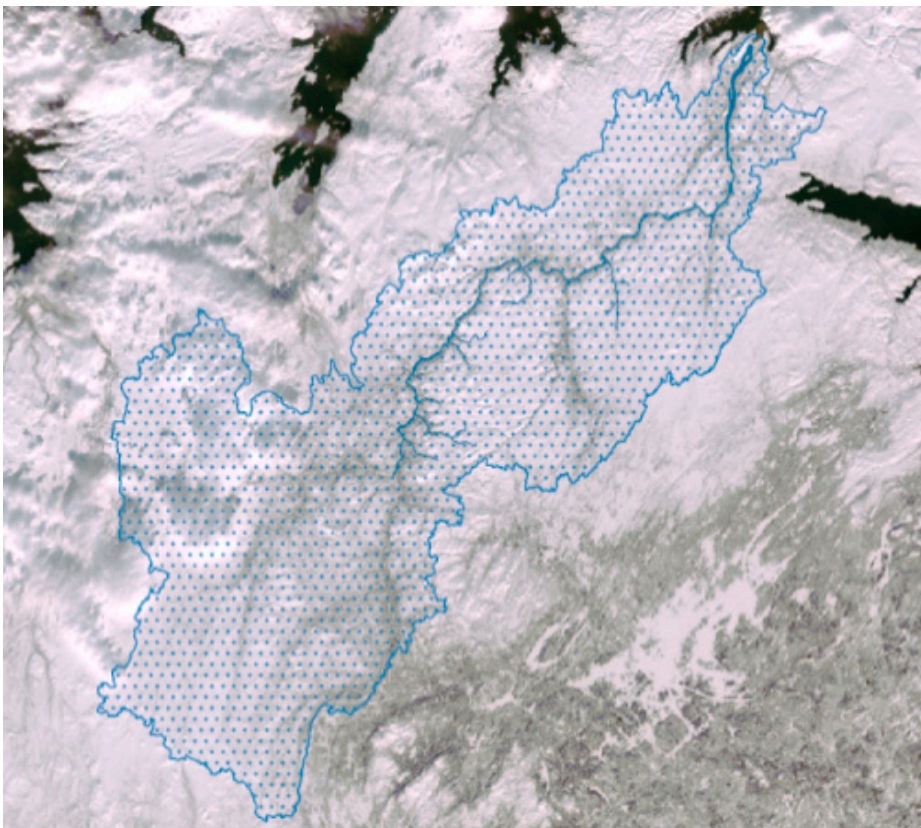


Figure 6. Sentinel-3 (OLCI) true-colour image (2019-03-22) and the catchment area of the Tana river.

The Sentinel-3 A and B satellites of the European Space Agency (ESA) have the optical OLCI instrument, which provides a large-scale imagery with almost full coverage of the Earth each day. Another example providing daily acquisitions are the Aqua and Terra satellites of NASA, which are equipped with the optical MODIS instrument. Although these satellites provide almost full daily coverage of the Earth, the spatial resolution is relatively coarse, ranging from 300 to 1,000 meters (or *medium resolution*). More detailed imagery can be obtained with Sentinel-2 (ESA) and Landsat-8 (NASA) satellites, which provide imagery with spatial resolutions of 10-30 meters (or *high-resolution*), the revisit time is slow; it takes 5-10 days for these satellites to cover all of the earth. For monitoring an area as large as the catchment zone of the river Tana, the medium resolution satellite instruments OLCI and MODIS with high temporal coverage are efficient tools providing valuable data and consistent time series.

To quantify the onset and duration of the melting period, the so-called Fractional Snow Cover (FSC) product is a standardized tool (FSC, 2021). FSC is a satellite derived measure for estimating the percentage of snow cover of an observed area (Figure 7).

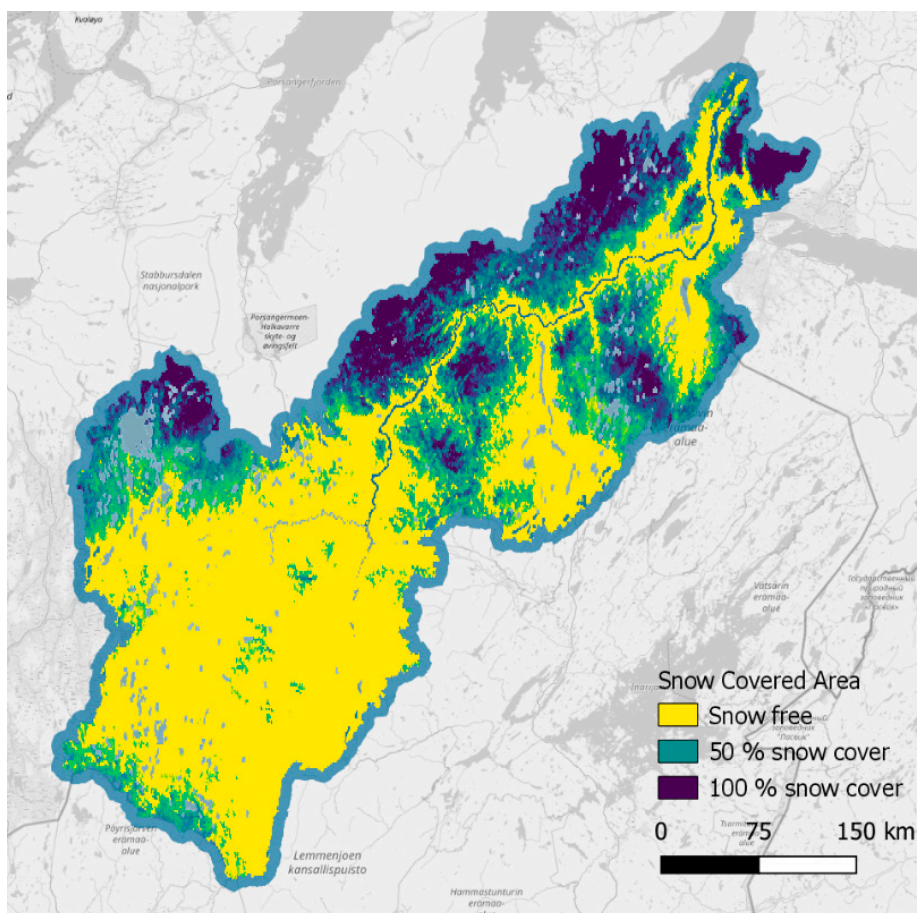


Figure 7. The Fractional Snow Cover derived from MODIS Terra (2017-06-11)

With the high temporal coverage of the medium resolution instruments, a solid time series can be produced about the snow coverage to estimate the intensity of the melting period each year (Figure 8). The differences between years are evident, which hints at the varying annual dynamics of the river.

Although the medium resolution satellite instruments provide the best spatial and temporal coverage, a more detailed view of the distribution of the snow cover is provided by the high-resolution instruments, e.g., Sentinel-2 MSI and Landsat-8 OLI. The snow coverage can be visualized effectively using the short-wave infrared band (SWIR) of the Sentinel-2 MSI instrument (Figure 9).

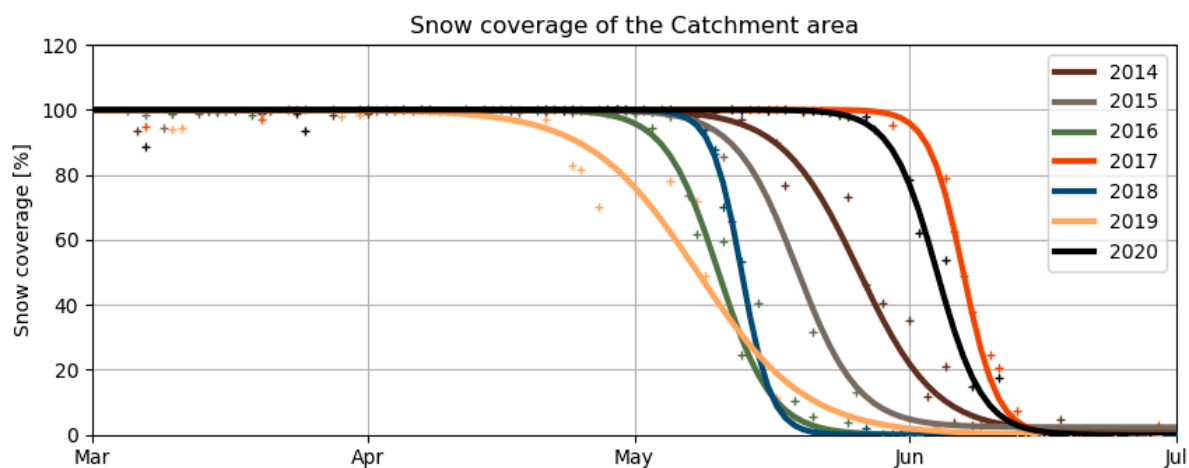


Figure 8. Percentage of the catchment area of Tana River covered by snow during March to June in separate years. The + symbols are satellite observations. The solid lines represent a fit with a sigmoid function.

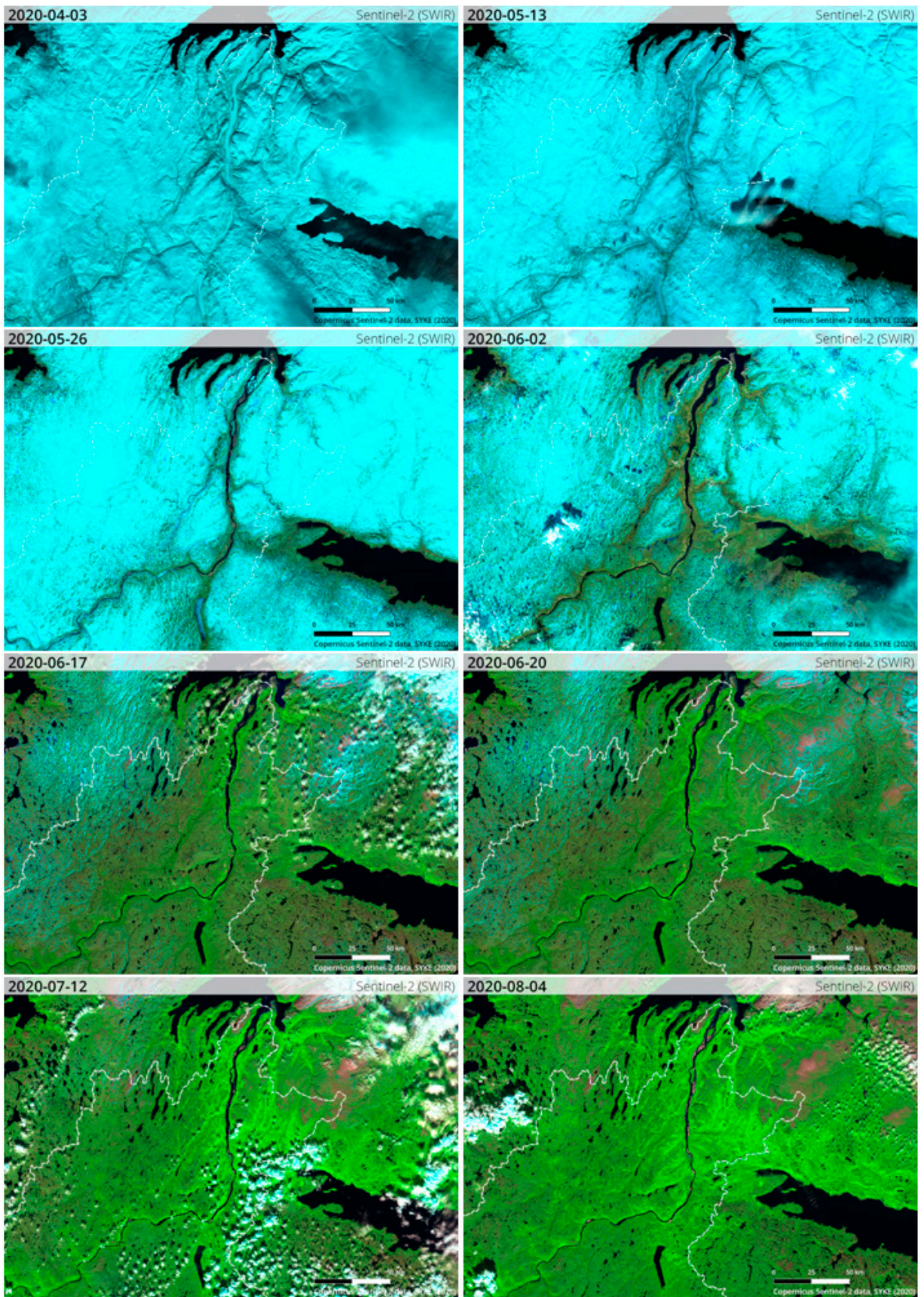


Figure 9. The snow cover of the Tana river catchment zone over the melting period in April-August in 2020. The images represent the SWIR-visualization of Sentinel-2 data, which indicates snow and ice in turquoise, vegetation in green and rock in brown. The white dashed line indicates the boundary of the catchment zone.

4 Early spring – Ice

Each winter the Tana river is covered completely by ice and snow, all the way up to the river delta. The ice cover of the river can easily be estimated from the true colour images. The open water is rendered dark, but snow and ice are very bright as they reflect most of the sunlight back, which gives a strong contrast between the open water and ice-covered water.

As the river is quite narrow in width (100 m to 1 km), the medium resolution satellites are not able to capture a detailed enough view of the river ice cover, but the high-resolution satellite Sentinel-2 can monitor the landscape with a resolution of up to 10 meters, allowing a very detailed view into the river ice. In 2020, the ice run happened later than previous years (at the end of May) and was very abrupt (Figure 10).

Although the ice cover can easily be estimated by visual inspection, remote sensing provides an efficient tool to automatically quantify the ice cover over time. Based on the differences between the light reflected at different parts of the spectrum, the so-called Normalized Difference Snow Index (NDSI) can be computed from each satellite overpass (NDSI, 2021). This index can be used to automatically classify the different parts of the river based on whether the river area is covered by or is free of ice or snow (Figure 11).

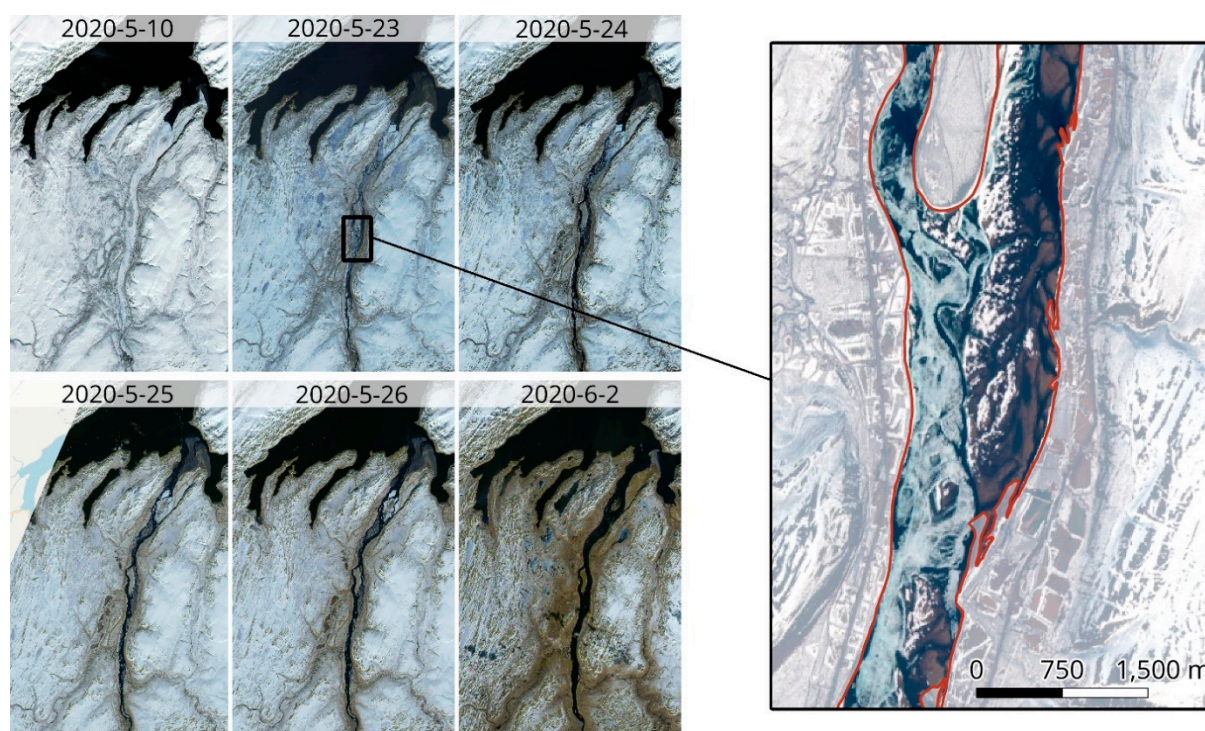


Figure 10. Left: Time series of true colour imagery of the ice run at the end of the Tana river in 2020 (Sentinel-2). Right: A close-up-view at a 10 meter spatial resolution (Sentinel-2, 2020-5-23).

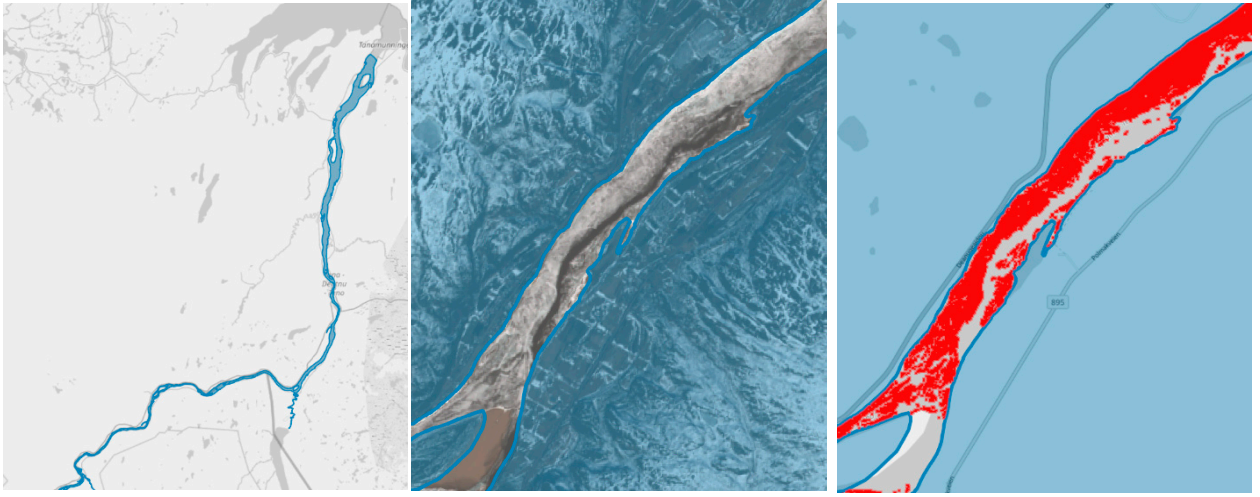


Figure 11. The bounding area of the river Tana (left), closeup (middle) and computed ice cover (right, red).

Using this methodology, the ice cover of the full river area can be monitored during the full melting period in each year. The onset time of the river ice melting differs from year to year, depending on the current weather cycle and the intensity of the catchment area runoff. When compared to the snow cover of the river catchment area, one can note that the river ice begins to disappear before the snow cover has receded by any substantial amount (Figure 12). This is expected, as most of the snow mass resides at elevated altitudes, which warm up and melt later than the riverside areas. As the snow cover begins to melt, river ice is swept away almost a month prior to the snow cover.

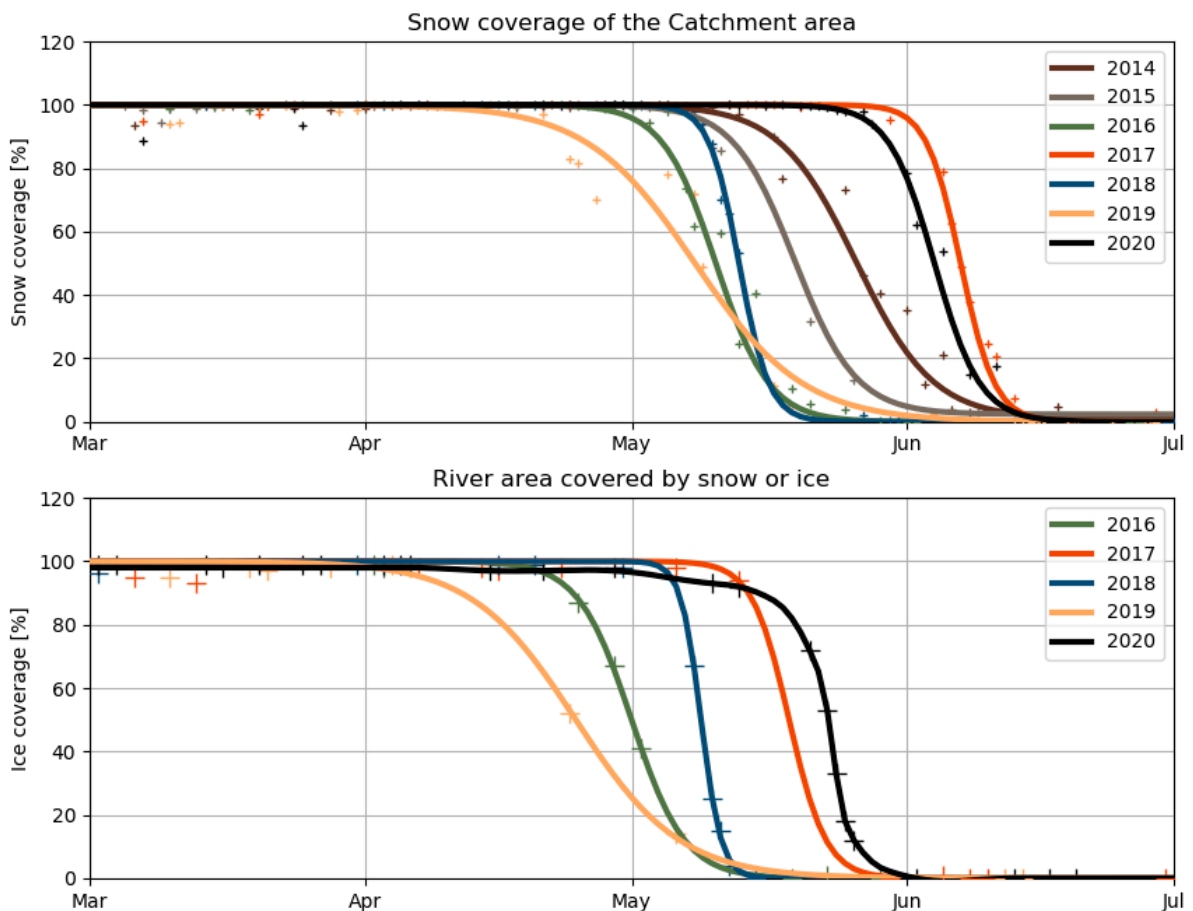


Figure 12. Percentage of the catchment area of the Tana River covered by snow, and the percentage of the river area covered by snow or ice during the melt periods in 2014-2020.

Later in the melting period, the ice cover has reduced, and the remaining river ice may become mobile due to strong currents caused by the snowmelt runoff. Then, ice dams might be formed along the river causing flooding of the nearby areas (Figure 13). Satellite based ice detection can be utilized to identify locations at an elevated risk of flooding.



Figure 13. Identification of a possible site for ice dam formation (Landsat-8 2018-05-13).

5 Late spring – Plumes

As the spring advances, more and more snow melts in the mountains, and the river network captures the runoff water. The Tana River collects the meltwaters of the surrounding catchment area, and as the melting progresses the river routes the meltwater to the Barents Sea. Large water masses during the melting period sever the sediments from the sand-based riverbed and transport the mobile sediment along with the flowing water until the sediment discharges into the Barents Sea at Tanamunningen. This phenomenon can be observed as large plumes of turbid water at the end of the Tana river during the most intense melting period (Figure 14).

As was the case with the snow and ice cover, the plumes can be inspected visually using true colour images. However, the remote sensing observations can be used to estimate the actual concentration of the suspended matter discharging from the river. The concentration can be computed by estimating the inherent optical properties (IOPs) of the water mass. This estimation is based on the known characteristics of how light is attenuated in water under different conditions: clear (“transparent”) water has different attenuation characteristics from those of turbid water. When these IOPs of the water base are known, concentrations of various classes of suspended matter (e.g., suspended solids, chlorophyll) can be estimated. The state-of-the-art methods for retrieving the IOPs of the water base from remote sensing observations are based on neural networks (e.g., the C2RCC-processor; Brockmann, 2016). These methods can be used to quantify and measure the impact areas of the river discharge, and to estimate the concentration of the suspended matter, i.e., turbidity, within the discharged water (Figures 15, 16 and 17).



Figure 14. A turbid plume of discharge water into the Barents Sea at the end of the Tana River, at Tanamunningen (Landsat-8 2018-05-13).

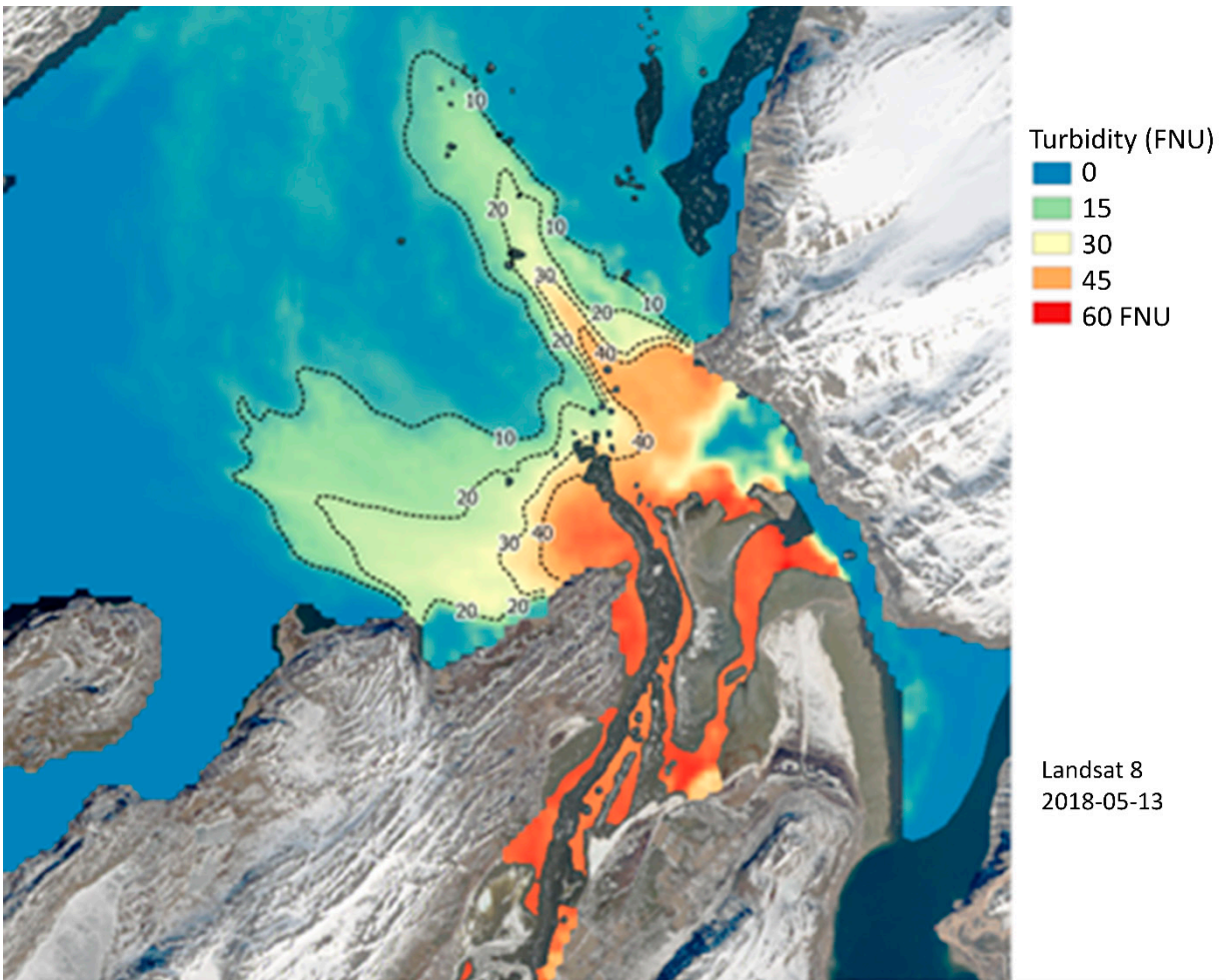
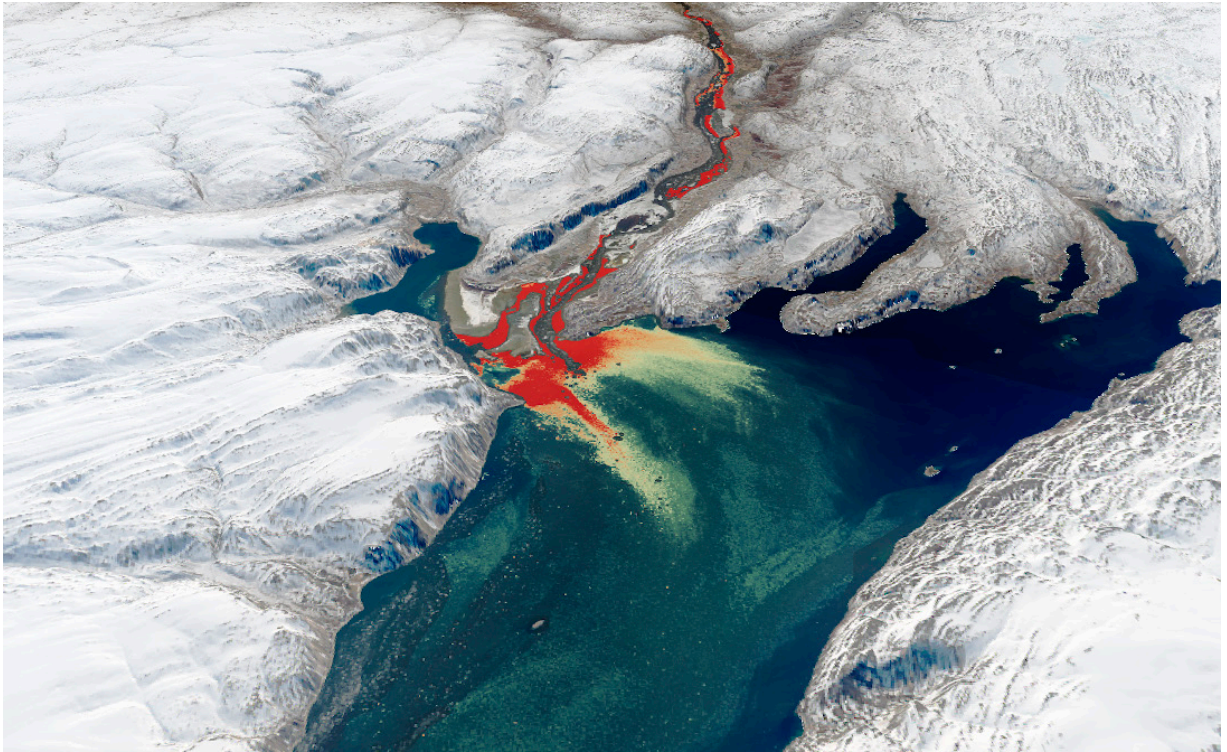


Figure 15. Satellite derived turbidity concentration of the discharge water into the Barents Sea at the end of the Tana river, at Tanamunningen (Landsat-8 2018-05-13).

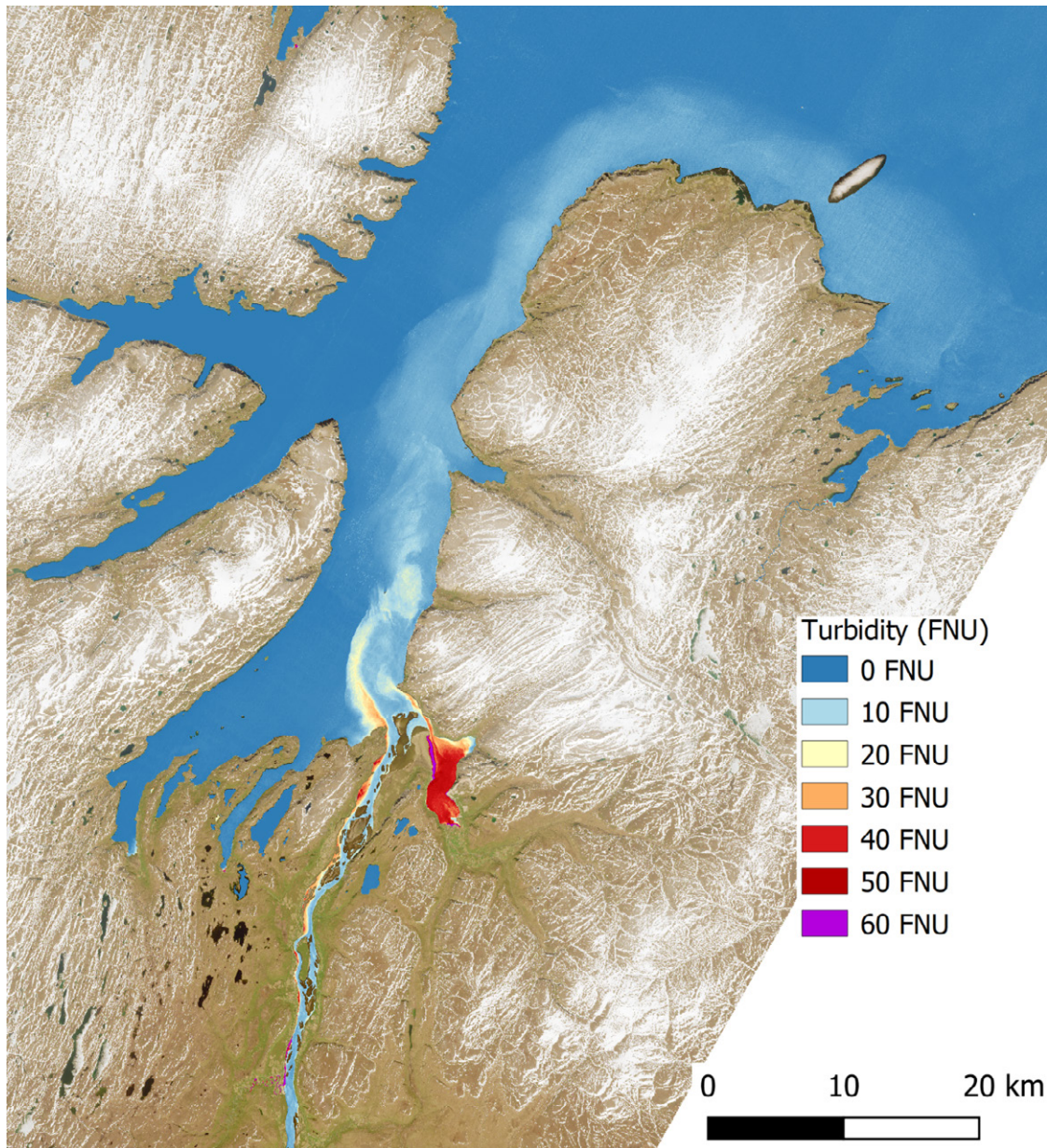


Figure 16. Satellite derived turbidity concentration of the discharge water into the Barents Sea at the end of the Tana river, at Tanamunningen (Sentinel-2, 2020-6-13). The plume of turbid water on the left side of Tanamunningen discharges from the Báisjohka river and extends all the way out into the Barents Sea.

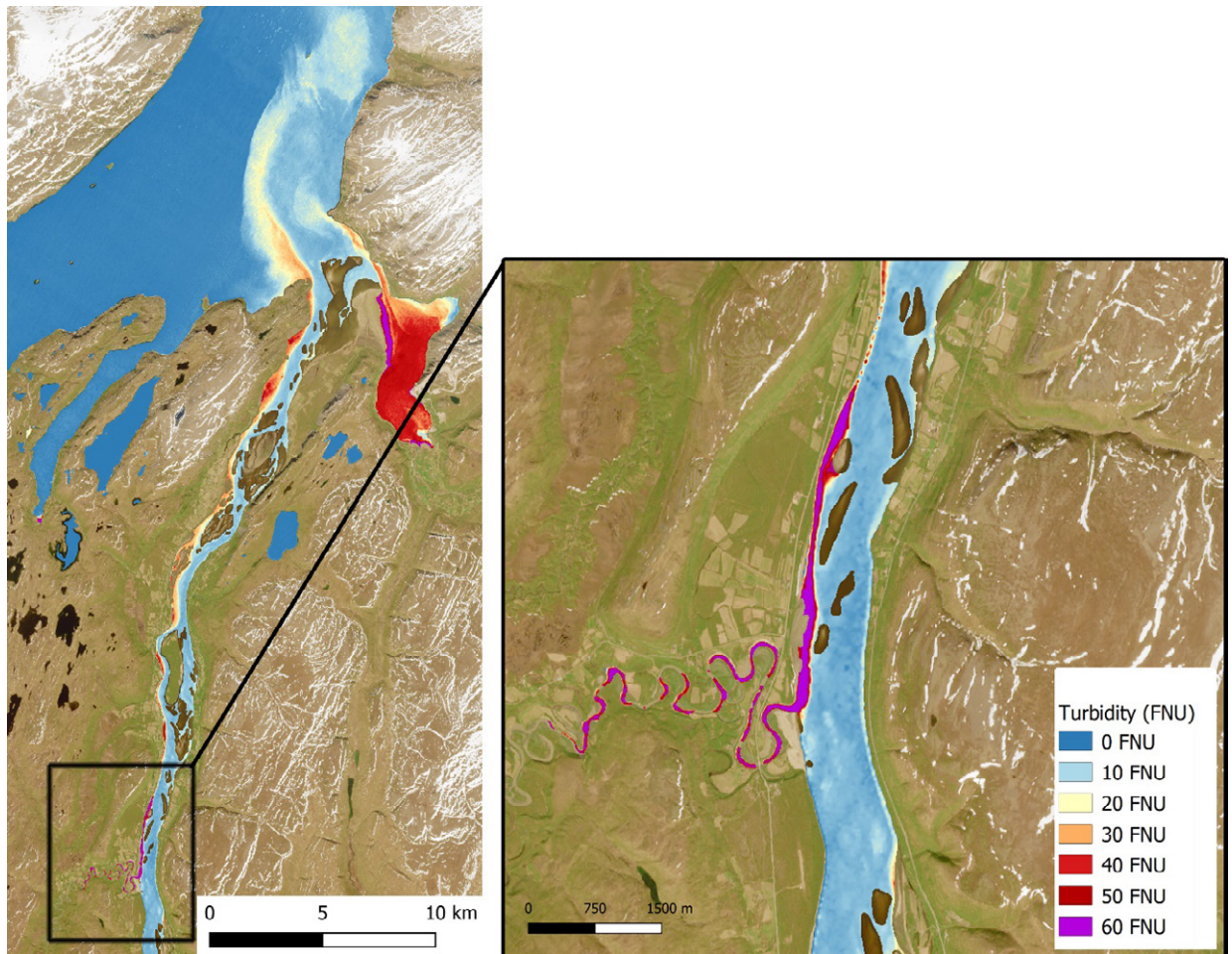


Figure 17. Satellite derived turbidity concentration of the discharge (Sentinel-2, 2020-6-13). Close up of the discharge point of the Báisjohka river.

6 Early summer – Warming water

As the summer begins and all the ice and snow are finally gone, the remaining water warms up. During the melting period the river water is mixed with ice at temperatures close to zero °C and remains cold until all the ice has retracted. However, the water mass beyond the river discharge area is free from ice through the winter and begins to warm up already during spring.

Some satellites have temperature sensors on board, most notably Sentinel-3 with the medium resolution SLSTR instrument, and Landsat-8 with a higher resolution TIRS instrument. The advantage of the satellite-based temperature estimate to the in-situ measured temperature is that the temperature measurement is not restricted to a single location—instead a full coverage of the temperature distribution over an area is obtained at once (Figure 18).

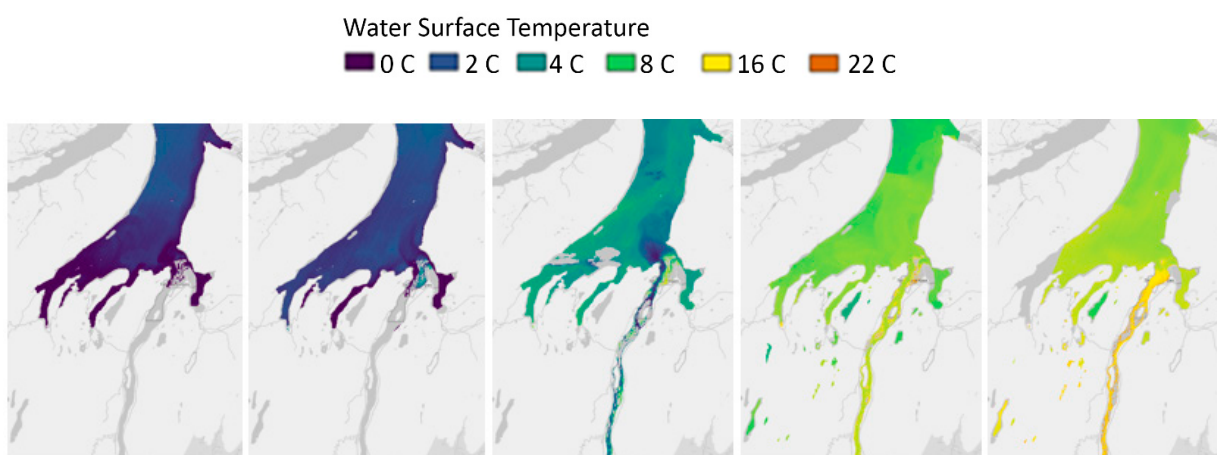


Figure 18. Water surface temperature at Tanafjord, in the Barents Sea (Landsat-8 2019-03-20, 2019-04-05, 2019-05-07, 2019-06-15 and 2019-07-12).

With the satellite derived temperature data, the temperature differences between the discharge water and the main receiving water body can be evaluated. For example, during the intense melting period in 2018, the water discharging from the river delta was about five degrees Celsius below the temperature of the surrounding water mass—which was a cold water region penetrating about 15 km into Tanafjorden (Figure 19).

The temperature estimation can be extended to any water body covered by the satellite overpass. Near the Tana River a group of small lakes exist at different altitudes. Their temperatures can readily be estimated during each satellite overpass (Figure 20).

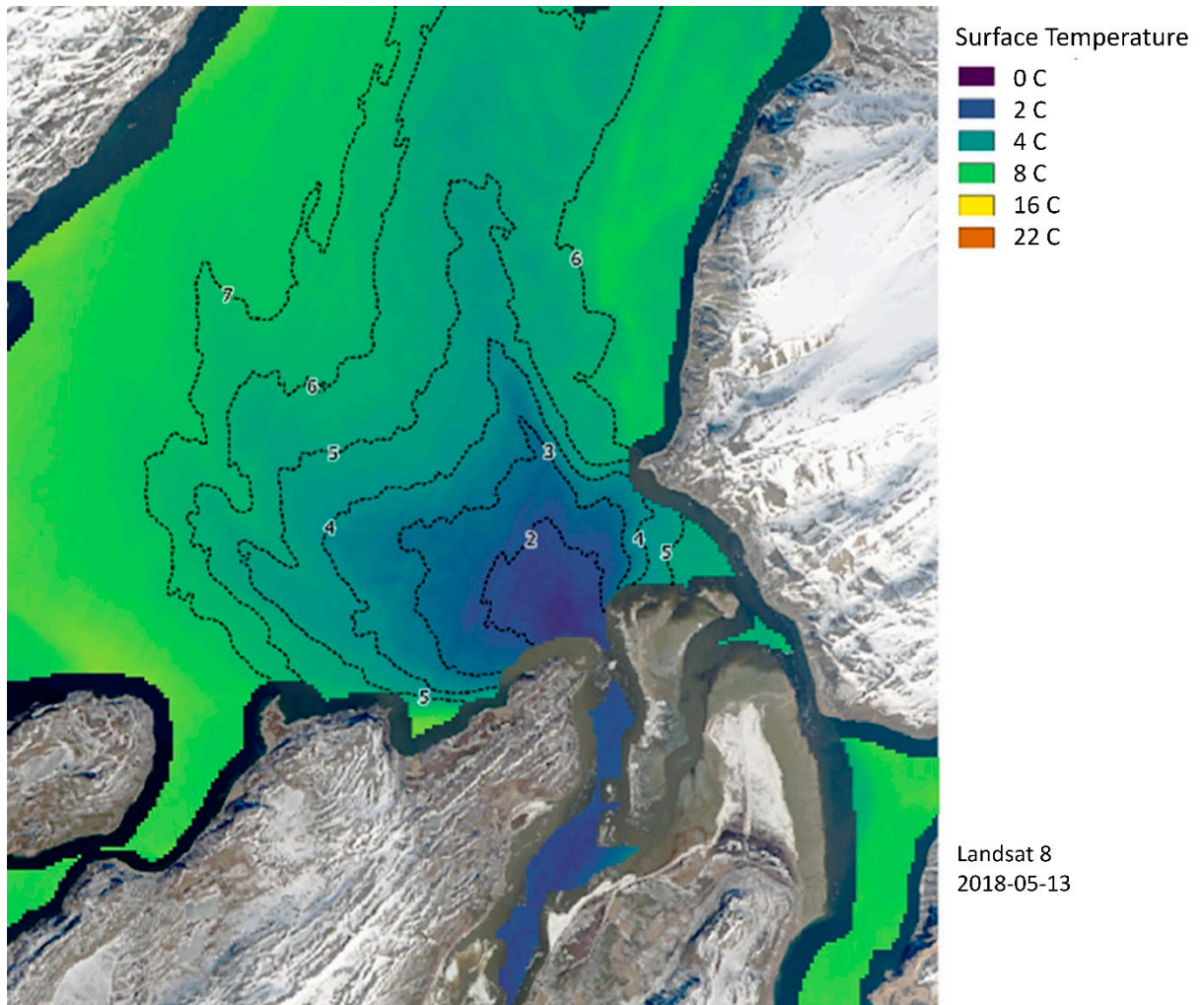


Figure 19. Water surface temperature of the discharge water in May 2018 (Landsat-8).

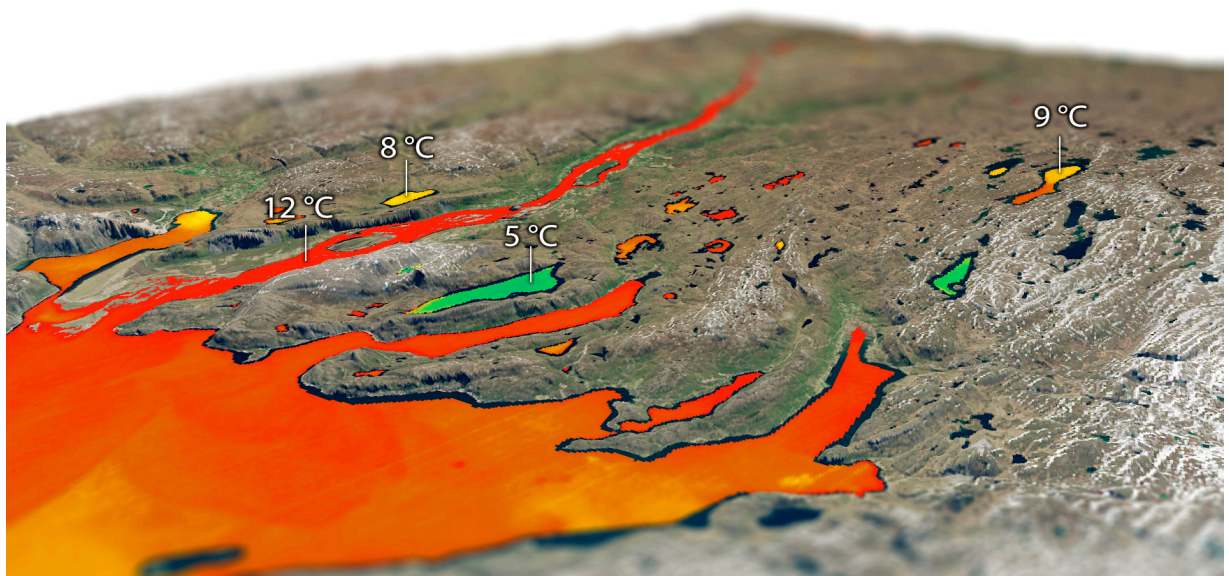


Figure 20. Water surface temperature of the lakes at different altitudes near the Tana river (Landsat-8 2019-06-15).

7 Late summer – Retreating water

Further into the summer, the river flow gradually decreases, and the river dries out, finally ending up with only a narrow stream meandering through the river valley. The drying river reveals the sand banks of the river delta and the riverbed becomes exposed (Figure 21).

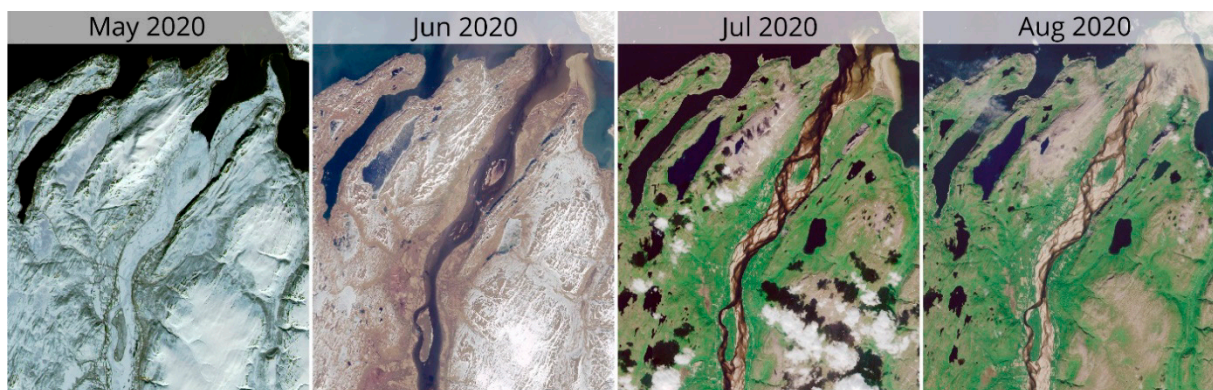


Figure 21. Time series of true-colour images illustrating the changes in water content of the river (Sentinel-2).

After the spring flooding, the amount of remaining water mass depends on a variety of factors: the duration of the snowmelt at the catchment zone, the annual rainfall intensity and changes in the average temperature. A pair of true-colour images from July 8th in 2017 and 2019 illustrate how the onset date of the annual melting period affects the river (Figure 22). In 2017, the melting period began a full month later than in 2019, giving the river significantly less time to recover from the meltwater flooding. The water levels in late-snowmelt-year 2017 are significantly elevated when compared to early-snowmelt-year 2019.

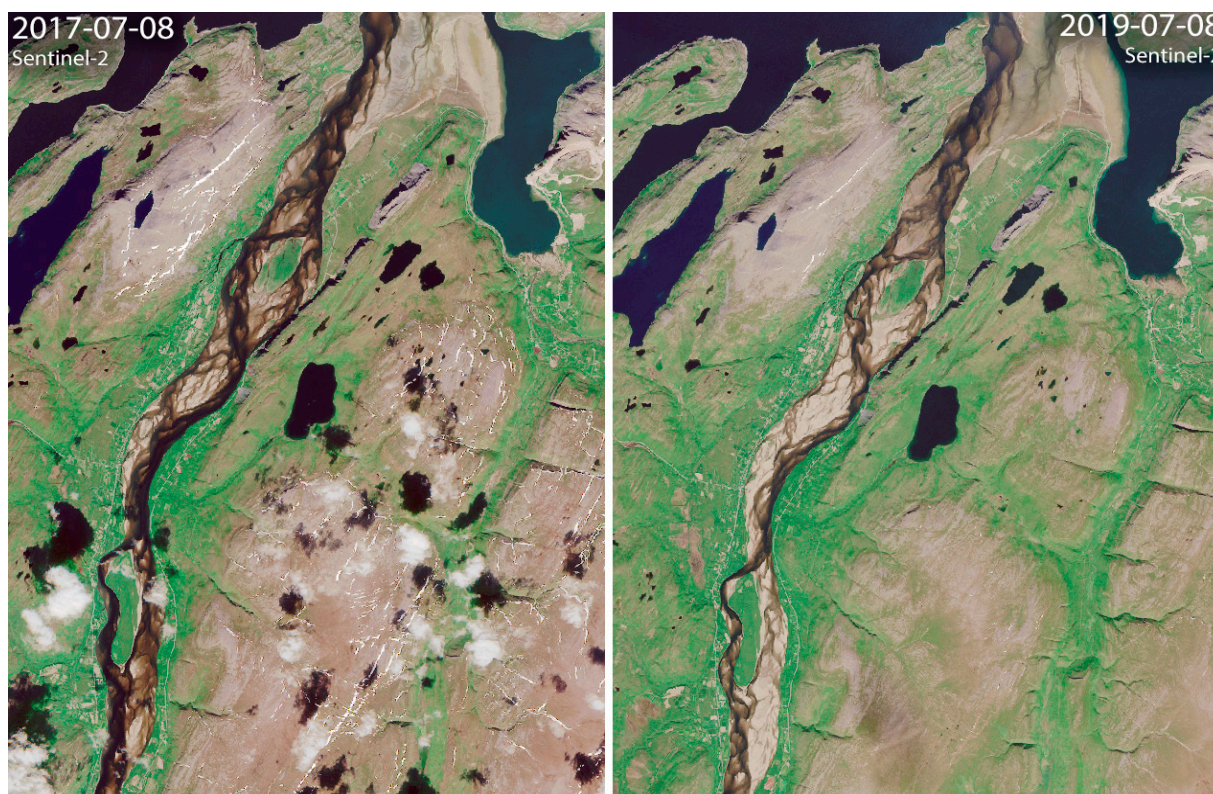


Figure 22. True-colour images illustrating the differences in water content of the river in different years.

As with the ice cover, the river area covered by water can be estimated from the satellite data. The dry land and wet water have different properties related to how they reflect light—dry land reflects light more strongly than water. This forms a basis for the so-called *Normalized Difference Water Index* (NDWI). The NDWI is a measure of the water content of the area that the satellite observes and can be used to estimate the water covered area of the river (Figure 24 and Figure 25). Similarly to snow cover in the drainage basin and in the river, it is possible to compute time series of this parameter (Figure 23).

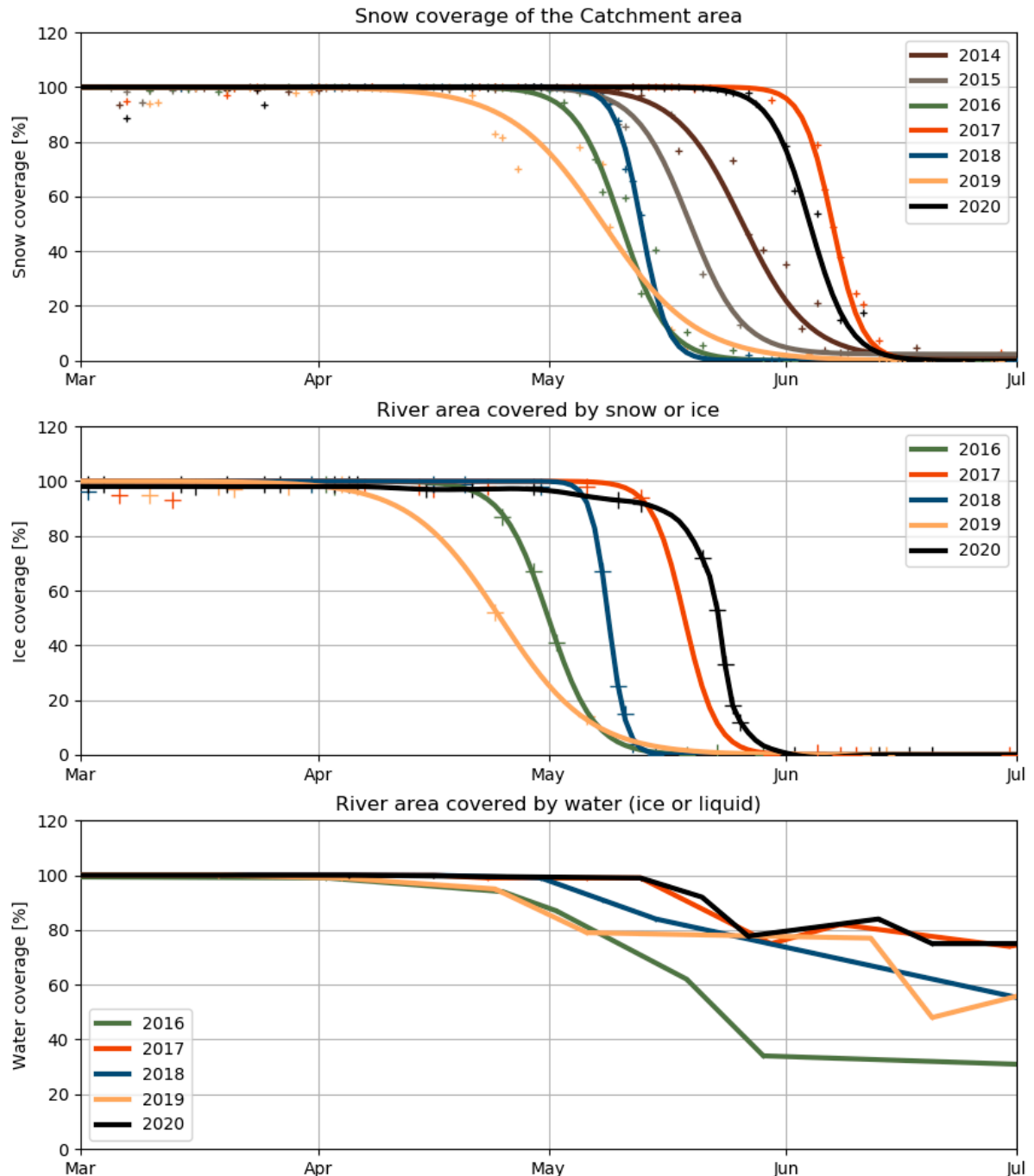


Figure 23. Percentage of the catchment area of the Tana River covered by snow, the percentage of the river area covered by snow or ice and the percentage of the river covered by water during spring periods in 2014-2020.

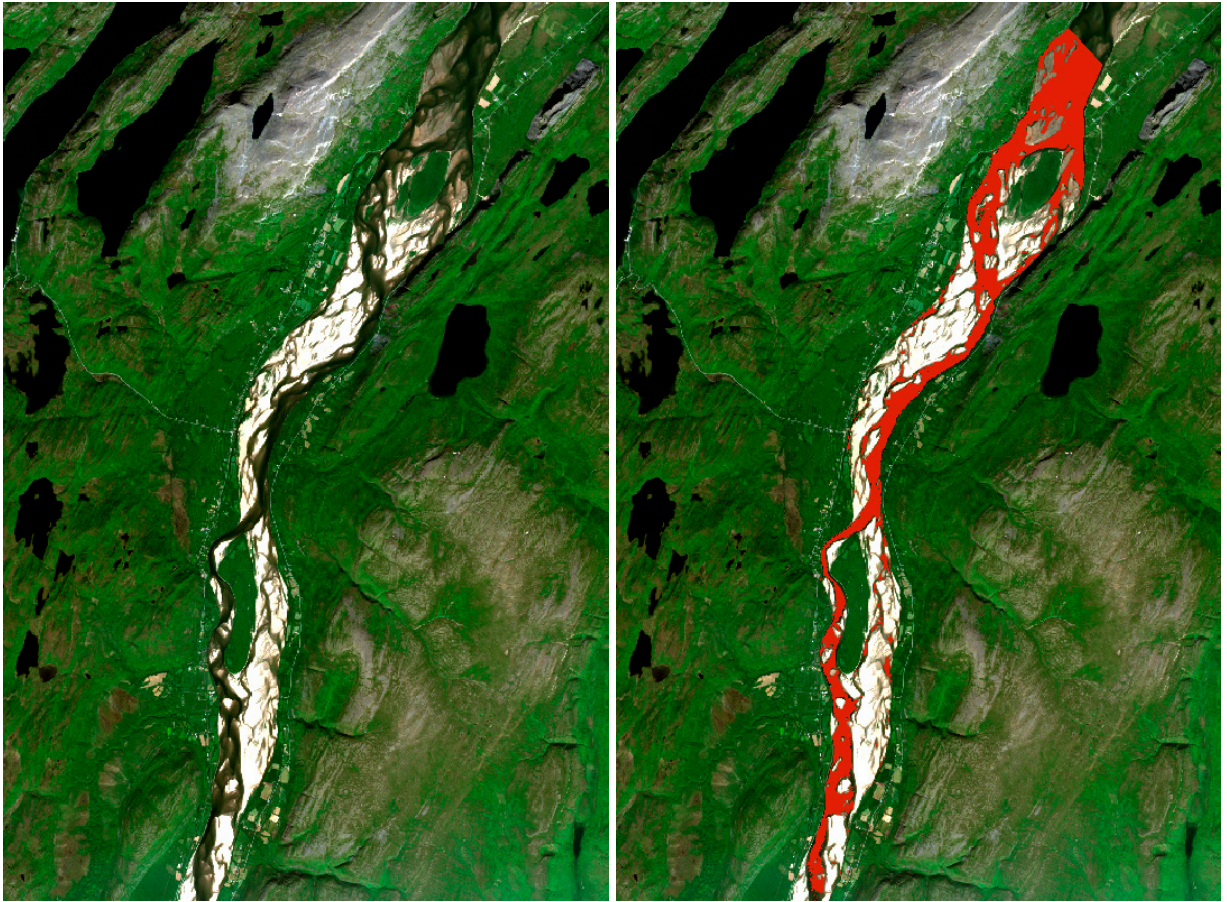


Figure 24. True-colour image (left) and automatically identified water areas (right, red). Sentinel-2, July 18, 2017.

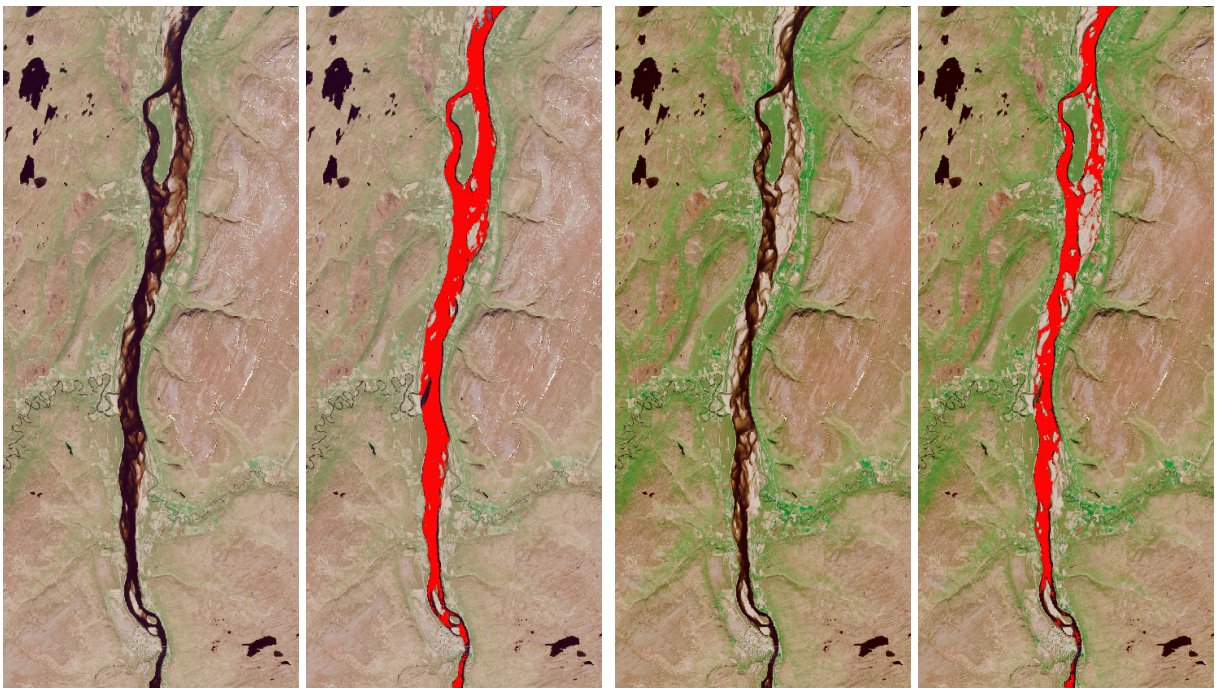


Figure 25. Coverage of the river water change between June 15th (left) and 21st (right) in 2019 by Sentinel-2.

The true-colour satellite imagery illustrates how the sea or riverbed structure is visible during clear water conditions, because the water column above does not completely absorb all the light (Figure 27). The satellite instruments observe the light reflection from both the water and the bottom, revealing the bumps and valleys below the water surface. This phenomenon is most notable for water bodies with a sand-based bottom, because sand is a relatively good light reflector—on the other hand, macrophytes or other “dark matter” on the seabed absorb the remaining light and leave less visible reflections. The light is completely absorbed by the water as well when the water column height increases.

However, under the conditions when enough light is reflected from the bottom (at depths of ca. 2-10 meters with a highly reflective seabed), an estimate can be produced of the height of the water surface. The water absorbs relatively little light at the blue part of the spectrum (small wavelengths), while the absorption increases as the wavelength increases towards the red end of the spectrum. Therefore, at shallow depths, the difference between the bottom-reflections at different wavelengths relates to the height of the water column, giving the opportunity to use satellite data for bathymetric mapping, or Satellite Derived Bathymetry (SDB; Traganos et al., 2020).

The high flow rates through the river during the melting period shape the bottom bathymetry as the sand is eroded by the water. Satellite derived bathymetry can be used to monitor these changes over longer time periods, and to construct bathymetric maps (Figure 26).

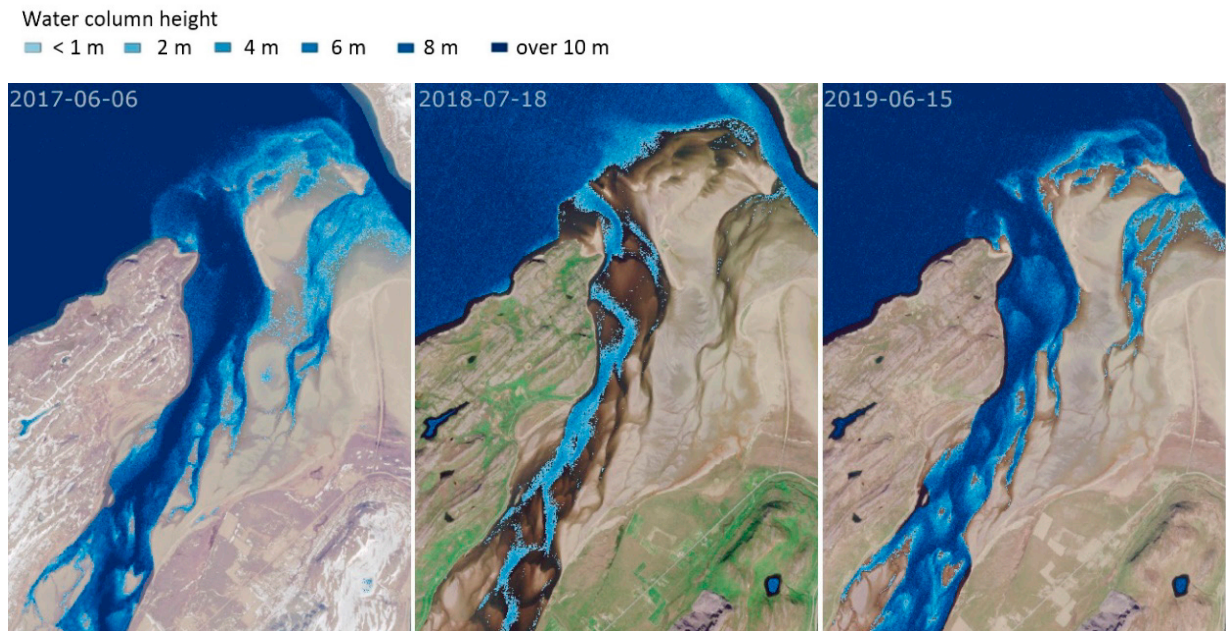


Figure 26. Water surface height from the bottom at 2017-06-06, 2018-07-18 and 2019-06-15 (Sentinel-2).



Figure 27. True-colour image of Tanamunningen on 2019-06-15 showing the sandy river bottom during the low water season (Sentinel-2).

8 Further actions

The main objective of the project and this report was to promote the use of EO for providing information about the state and changes of the Arctic environment. The results presented here demonstrate the advantages and capabilities of satellite-based observations. EO methods can provide spatially and temporally extensive data about several variables relevant to the Arctic and detailed new information about the processes taking place in the Arctic.

The proposed next steps are to extend the use of EO methods into efficient routine use for monitoring the arctic environment. The provision of EO-based lake ice, snow cover and water quality information is already ongoing and partially automated. Additional effort is needed especially for the following:

- **Further processing of EO-based information:** Automate the provision of various compilations and analyses.
- **User collaboration:** Provision of training material and guides, organization of training events, and identification and development of additional use cases together with users.
- **Identification of barriers:** National legislation and security policies may hinder the utilization of EO methods. These need to be identified.

Acronyms

EO	Earth Observation
LC8	USGS/NASA Landsat-8 satellite
NDSI	Normalized Difference Snow Index
NDVI	Normalized Difference Vegetation Index
NDWI	Normalized Difference Water Index
OLCI	Ocean and Land Colour Instrument
S2	ESA Copernicus Sentinel-2 satellite
S3	ESA Copernicus Sentinel-3 satellite
SDB	Satellite Derived Bathymetry
SLSTR	Sea and Land Surface Temperature Radiometer

References

- AMAP 2017. Snow, Water, Ice and Permafrost in the Arctic - Summary for Policy-makers. <https://www.amap.no/documents/download/2888>
- Brockmann, C., Doerffer, R., Peters, M., Stelzer, K., Embacher, S., Ruescas, A. 2016. Evolution of the c2rec neural network for sentinel 2 and 3 for the retrieval of Ocean colour products in normal and extreme optically complex waters. Living Planet Symposium 2016', Prague, Czech Republic, 9–13 May 2016 (ESA SP-740, August 2016)
- ELY-centre for Lapland 2010. The preliminary flood risk assessment in Tana River basin. <https://www.ymparisto.fi/download/noname/%7B1D827398-71CB-4D79-B103-C4EEE552BAC7%7D/78144>
- FSC 2021. Fractional Snow Cover for the Northern and Central Europe. SYKE. <https://ckan.ymparisto.fi/dataset/%7B36B533E7-FCFB-49FD-802B-1AC37968B057%7D>
- MET Norway 2020. The Norwegian Meteorological Institute open data.
- NDSI 2021, Sentinel-2 image index mosaics, NDSI. SYKE. <https://ckan.ymparisto.fi/dataset/%7BE389EAB4-6143-43BC-9D64-0C2CBE025D71%7D>
- Traganos D., Foursanidis D., Aggarwal B., Chrysoulakis N. 2020. Estimating Satellite-Derived Bathymetry (SDB). Remote Sensing 10(6):859, DOI 10.3390/rs10060859
- TARKKA 2021. TARKKA map service for satellite images. SYKE. <https://ckan.ymparisto.fi/dataset/%7B78DE3DBB-18AF-4D0C-9833-8D97178B8EB0%7D>. (The service can be accessed online at <https://syke.fi/TARKKA>)
- True-colour satellite images 2021. SYKE. <https://ckan.ymparisto.fi/dataset/%7B7DADB718-EE96-4E9B-B7A3-EBC4A922AA38%7D>



ISBN 978-952-11-5523-9 (PDF)

ISSN 1796-1726 (online)